# Determination of the Buckling Critical Load for Composite Concrete-Filled Steel Tube Columns from Partial Experimental Data: A Review of the Southwell Plot Technique

Tiziano Perea[1], Roberto T. Leon[2], Mark D. Denavit[3], Jerome F. Hajjar[4]

## Abstract

This paper discusses two techniques that target the determination of the buckling critical load for composite concrete-filled steel tube (CFT) cantilever columns from partial or incomplete experimental axial load – lateral displacement ($P$-$\Delta$) data. The numerical techniques evaluated in this study are the secant approach (better known as the Southwell plot) and the tangent approach. The motivation of this study arises from the inability of a sophisticated laboratory system to reach the experimental peak buckling capacity of some full-scale composite CFT specimens during compression tests. The review of these two techniques is validated against an experimental dataset of CFT specimens. In addition, these two techniques are evaluated through numerical nonlinear analysis of composite CFT columns with different values of slendernesses and initial imperfections. The evaluation with both the available experimental dataset and the parametric study confirms the scope and limitations of these two techniques. The application of the secant approach allows a more accurate determination of the critical load for those composite CFT columns where the laboratory system is not capable to reach their buckling capacity.

## 1. Introduction

Perea (2010) conducted a comprehensive experimental research program on composite concrete-filled steel tube (CFT) columns that consisted of tests on eighteen full-scale slender specimens in a fixed-free configuration. The specimens were tested under a series of unique loadings that included buckling loads, combinations of different axial and transverse loads inducing both uniaxial and biaxial bending, and torsional load histories. The description of the test series and the main experimental results with respect to buckling loads are documented in Perea *et al.* (2013).

---

[1] Professor, Universidad Autónoma Metropolitana – Azcapotzalco, <tperea@azc.uam.mx>
[2] David H. Burrows Professor, Virginia Polytechnic Institute and State University, <rleon@vt.edu>
[3] Assistant Professor, University of Tennessee, Knoxville, <mdenavit@utk.edu>
[4] CDM Smith Professor and Chair, Northeastern University, <JF.Hajjar@northeastern.edu>

These specimens were tested at the Multi-Axial Subassemblage Testing (MAST) Laboratory of the George E. Brown, Jr. Network for Earthquake Engineering Simulation (NEES), a large universal testing machine with precise six degree-of-freedom (DOF) control of both load (forces and moments) and deformation (displacements and rotations) at the top crosshead (Hajjar *et al*. 2002). The crosshead capacity for axial loadings in the MAST system has a nominal value of 5,872 kN (1,320 kip), which is constrained by the 1,468 kN (330 kip) capacity for each of the four vertical actuators that are connected to the crosshead.

The first load case in the load protocol consists of moving the crosshead with an incremental downward vertical displacement ($\Delta_z$) and with free lateral translation ($\Delta$) and free rotations ($\theta$) controlled at the top. Both principal translations ($\Delta_x$ and $\Delta_y$) and rotations ($\theta_x$ & $\theta_y$) were controlled as free in the circular specimens ($K_x = K_y = 2$), while in the rectangular specimens the y-axis was kept fixed ($\Delta_y = \theta_y = 0$) and only the x-axis was controlled free ($K_x = 2$, $K_y = 0.5$).

In four of the eighteen specimens in this test matrix, the expected axial buckling critical load was larger than the axial capacity of the MAST system. These four specimens include two circular specimens with 20-inch diameter (specimens 3 and 7) and two rectangular specimens with free translation towards the strong axis (specimens 5 and 9). The main characteristics of these four specimens are listed in Table 1. In this table, $L$ is the column length, $\lambda$ is the slenderness ratio, $P_n$, is the expected buckling load as per the AISC Specification (AISC 2016), and $P_{max}$ is the maximum experimental load applied to the specimen at the MAST system (limited to the maximum available capacity of the testing system). The geometric and material properties reported in Table 1 correspond to actual values measured and obtained from material testing.

Table 1. CFT specimens with a nominal compressive strength higher than the laboratory system

| Specimen | Steel | | Concrete | | $L$ (m) | AISC 360-16 | | $P_{max}$ (kN) |
| --- | --- | --- | --- | --- | --- | --- | --- | --- |
| | HSS | $F_y$ (MPa) | $f_c$ (MPa) | $E_c$ (GPa) | | $\lambda$ | $P_n$ (kN) | |
| 3 | HSS508×6.4 (HSS20×$^1/_4$) | 328 | 40.0 | 27.6 | 5.52 | 1.10 | 6295.5 | 5872[a] |
| 7 | | | 91.0 | 41.9 | 5.53 | 1.36 | 9088.9 | |
| 5 | HSS508×304.8×7.9 (HSS20×12×$^5/_{16}$) | 365 | 40.7 | 27.6 | 5.54 | 0.91 | 6528.0 | |
| 9 | | | 91.7 | 41.9 | 5.55 | 1.07 | 9513.4 | |

Note: [a] Maximum laboratory capacity to axial load.

Motivated by the fact that the compressive strength of these specimens cannot be determined directly from the experimental data, two techniques that target the determination of the buckling critical load of composite concrete-filled steel tube (CFT) columns from partial or incomplete experimental axial load – lateral displacement ($P$-$\Delta$) data are discussed and evaluated in the following sections.

## 2. Background

In the literature, there are methodologies that aim to estimate the unstable load based on the response with a lower load. Southwell (Horton *et al*., 1971) noticed a linear relationship between the ratio of lateral out-of-plumbness or out-of-straightness displacement to axial load ($\Delta/P$ or $\delta/P$) and the respective lateral displacement ($\Delta$ or $\delta$). He also noticed than the slope of that linear relationship is the inverse value of the buckling load. Similar linear relationships (Horton *et al*., 1971) were found by Ayrton and Perry ($1/P$ *vs*. $1/\Delta$), and by Donnel ($P$ *vs*. $P/\Delta$).

The first method, commonly referred as the Southwell plot, was initially developed by Ayrton and Perry in 1886, but later independently rediscovered by Southwell in 1932, and reexamined by Donnell in 1938. Horton *et al*. (1971) presented an historical review of this approach in its three available forms (Ayrton-Perry, Southwell and Donnell forms), as well as its derivation and some experimental validation. This method assumes that the first order terms in the series expansion solution derived for columns buckling elastically are predominant (so second order terms are neglected), and thus the axial force and the relative displacements can be represented by a linear relationship, where the elastic critical load is implicitly included (Timoshenko, 1961). Thus, a linear relationship will not be exhibited if the second order terms are considerable. These linear equations (Eqs. 1 to 3) can be plotted in different forms as illustrated in Figure 1, and as suggested by Ayrton-Perry (Eq. 1 for the relationship $1/\Delta$ *vs*. $1/P$), Southwell (Eq. 2 for the relationship $\Delta$ *vs*. $\Delta/P$) or Donnell (Eq. 3 for the relationship $P/\Delta$ *vs*. $P$). From these forms, the elastic buckling load is given by either the inverse of the initial abscissa from the Ayrton-Perry form, the reciprocal of the slope from the Southwell form, or the y-intercept from the Donnell form. Note that Southwell linear equation (Eq. 2) can be obtained by multiplying the Ayrton-Perry equation (Eq. 1) by the lateral displacement, $\Delta$. Similarly, the Donnell linear equation (Eq. 3) can be derived after some algebraic manipulation from either the Ayrton-Perry or the Southwell equations (Eqs. 1 and 2, respectively).



| (a) Ayrton-Perry form | (b) Southwell form | (c) Donnell form |
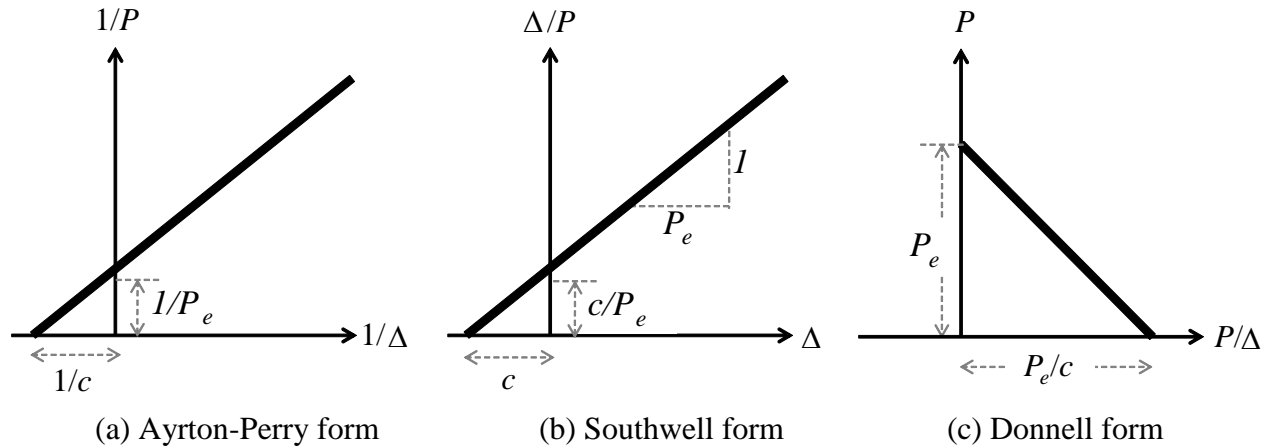
Figure 1. Linear relationship in columns with elastic buckling

$$\frac{1}{P} = \frac{c}{P_e}\frac{1}{\Delta} + \frac{1}{P_e} \qquad (1)$$

$$\frac{\Delta}{P} = \frac{1}{P_e}\Delta + \frac{c}{P_e} \tag{2}$$

$$P = P_e - c\frac{P}{\Delta} \tag{3}$$

As mentioned before, the previous approach (from now on just called Southwell or secant approach) is only valid in the elastic buckling range when the axial load and the axial load - lateral displacement ratio keep a linear relationship. In addition, this correlation is held linear only when relative displacements, $\Delta$, are used, but the relationship is not linear with the absolute displacements ($\Delta+\Delta_o$), and thus the effects of the initial imperfection, $\Delta_o$, are not included. Therefore, the application of this method is limited only to the determination of the Euler load, $P_e$.

The second method presented in this paper is based on the fact that, in either the elastic or the inelastic buckling ranges, the critical load is given when the tangent slope in the $P$-$\Delta$ curve reach zero. Thus, the plot axial force $P$ *vs*. $P$-$\Delta$ tangent, $dP/d\Delta$, is used (Figure 2(c)) for the determination of the buckling load. This approach accounts for both geometric imperfections and the material non-linearities (*i.e.* yielding in the steel, cracking and crushing in the concrete, Figure 2(a)). Similar to the Donnell form (Figure 2(b)), where the secant $P$-$\Delta$ is used for the estimation of the Euler load, $P_e$, the nominal critical load, $P_n$, from the tangent form is defined by its y-intercept or when the tangent becomes zero (Eq. 4).

$$P = P_n - c\frac{dP}{d\Delta} \tag{4}$$



(a) $P$-$\Delta$ curve          (b) Donnell (secant) form          (c) Tangent form
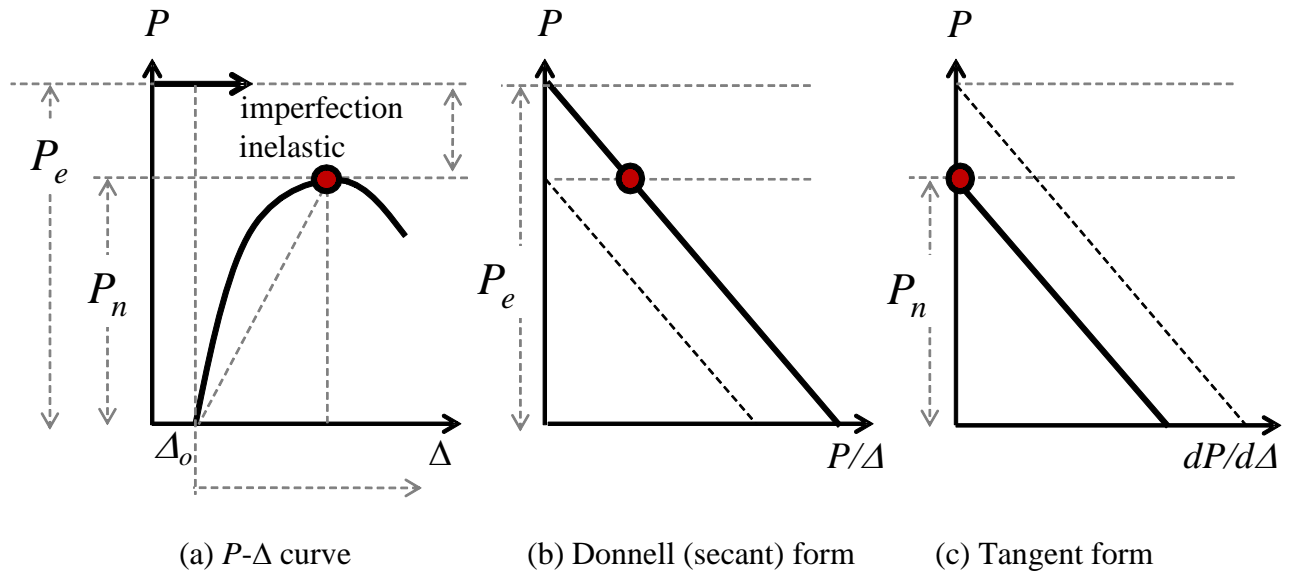
Figure 2. Proposed tangent form for elastic and inelastic buckling of columns

In this approximate method (from now on just called the tangent approach), the relationship *P-dP/dΔ* tends to be linear when the column remains elastic (elastic buckling range and low axial loads in the inelastic buckling range). In addition, geometric imperfections are included since the *P-Δ* slope follows the path defined by the initial imperfection (no matter if it is used relative Δ displacements or absolute Δ+Δ$_o$ displacements). As the load increases beyond the elastic limit for short columns within the inelastic buckling range, material nonlinearities (*i.e.* steel yielding, concrete cracking and crushing) change the tangent and the buckling load estimated linearly. Even if approximate, this method has some advantages over the Southwell plot.

In order to calibrate the accuracy of these approaches, the application of these methods to different analytical and experimental data results are presented and discussed in the following sections.

## 3. Analytical evaluation

Figure 3 shows the application of the tangent plot using data from analytical results. This data is obtained from a fiber analysis in a cantilever circular CFT column with nominal strength parameters. This column consisted of an HSS20.000×0.250 ASTM A500 Gr. B ($F_y$ = 289.6 MPa or 42 ksi) filled with concrete having a nominal strength of $f_c$' = 34.5 MPa (5 ksi). An initial out-of-plumbness imperfection of Δ$_o$ = *L*/500 was considered in the analysis. In addition, different slendernesses are used in these analyses. In these figures, $P_{cr}$ is the buckling load obtained from the analysis represented by the continuous line, and $P_t$ is the estimated load based on the tangent plot defined by two lower loads, defined by the points at 0.6$P_{cr}$ and 0.8$P_{cr}$, and represented by the dashed line. The prediction of the buckling load based on this method for these cases is reasonable, except for the shortest column shown in Figure 3(a).

Figure 4 shows the influence of the initial imperfection on the analytical results for the mentioned CCFT cross-section with a length of *L* = 5.5 m. (18 ft., λ = 0.97). The initial imperfections selected are *L*/250, *L*/500, and *L*/1000. As seen in this figure, the *P-dP/dΔ* curves tend to be linear for low axial loads, but the slope changes when the axial load approaches the buckling load. Changes in the slope seem to be lower for larger initial imperfections, where geometric nonlinearities are predominant. The predictions using the tangent form for these three cases are not exact (6% of maximum error), however, the critical load predictions, $P_n$, with this methodology are more accurate than the predictions obtained with the secant or the Southwell plot which are related to the Euler load, $P_e$.
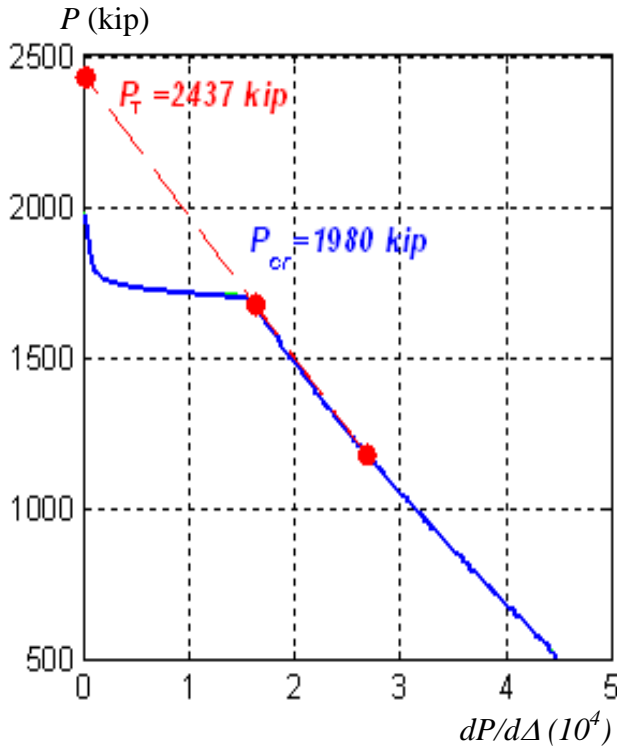
(a) $L = 2.7$ m. (9 ft.), $\lambda = 0.49$
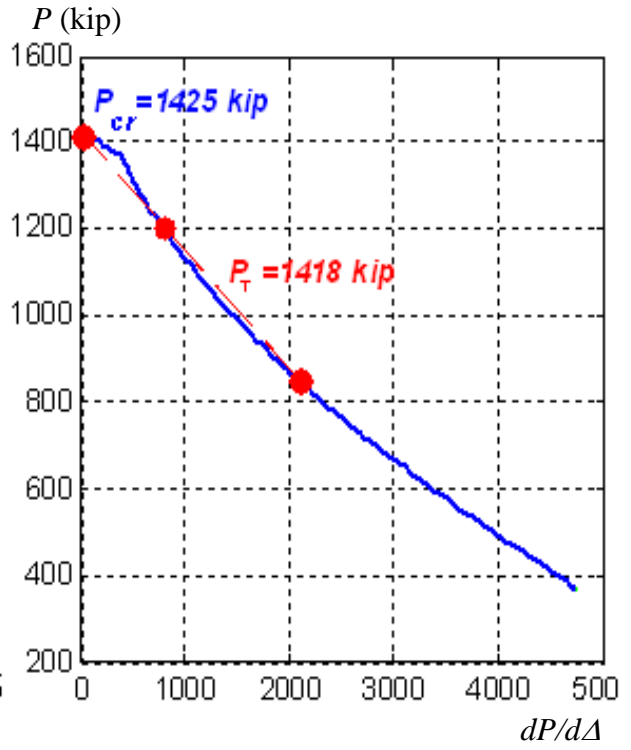
(b) $L = 5.5$ m. (18 ft.), $\lambda = 0.97$
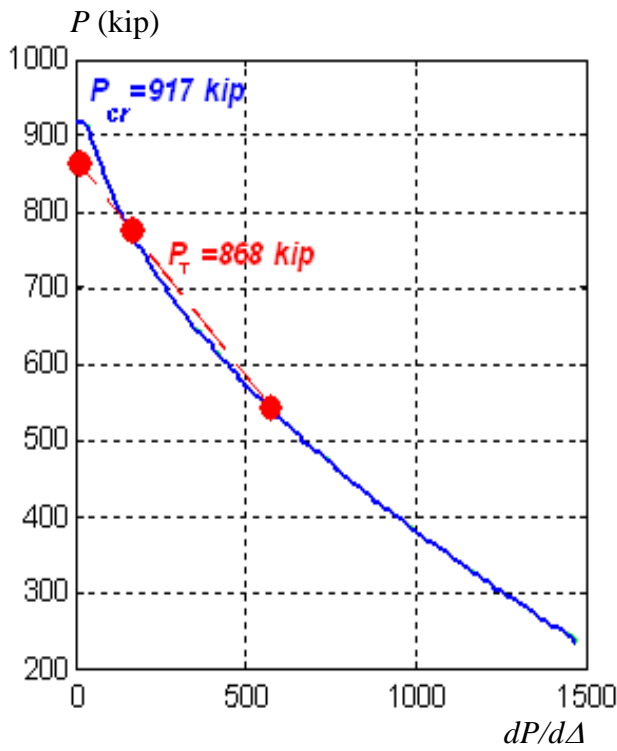
(c) $L = 7.9$ m. (26 ft.), $\lambda = 1.41$
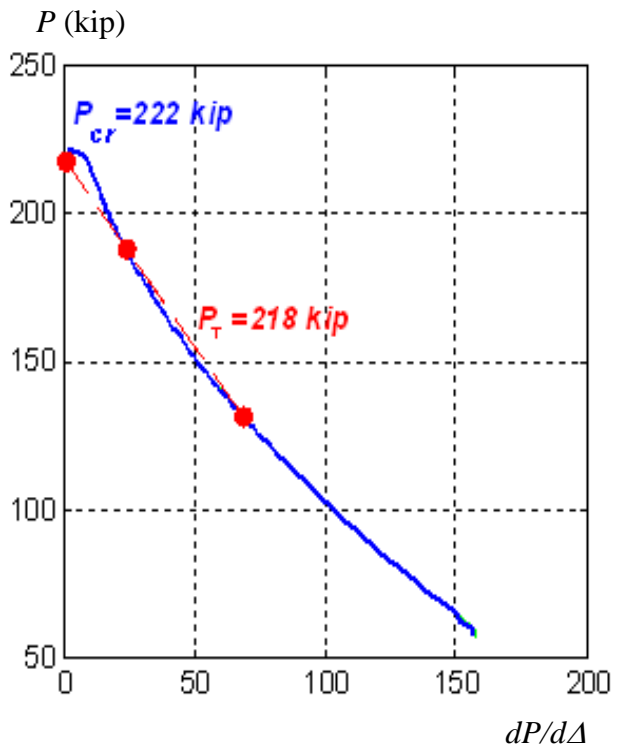
(d) $L = 16.8$ m. (55 ft.), $\lambda = 2.98$

Figure 3. Application of the tangent form on a CCFT column with different slenderness
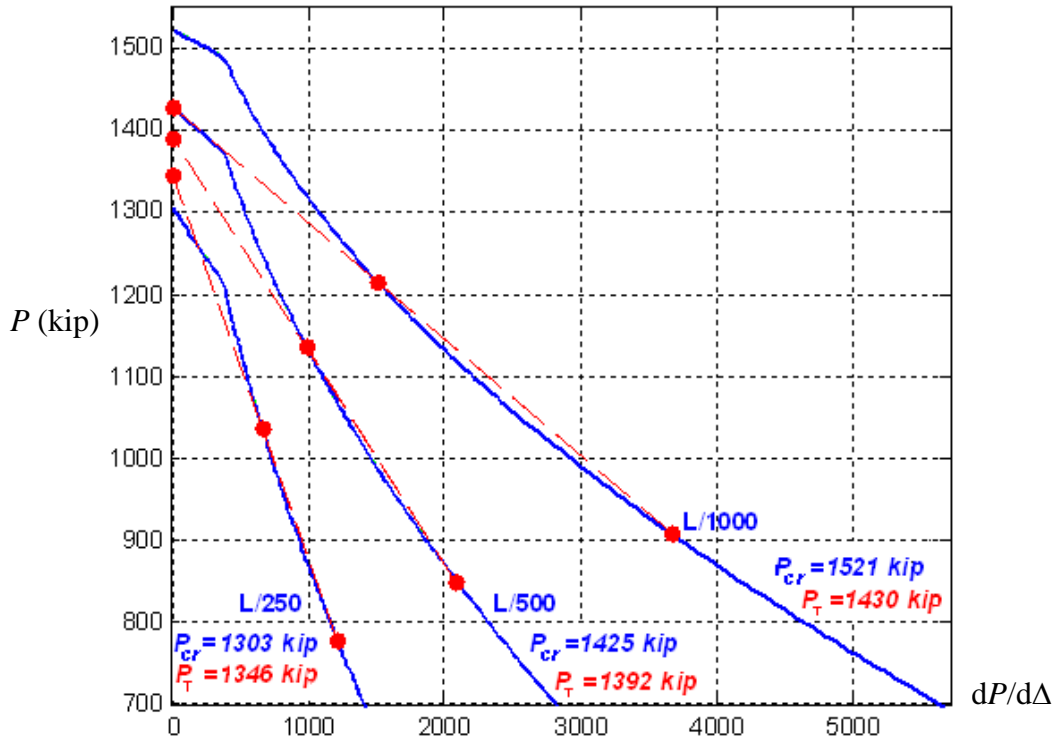
Figure 4. Application of the tangent form on a CCFT column with different imperfections

## 4. Experimental evaluation

As mentioned at the beginning of this section, the application of the secant plot (or Donnell form, variant of the Southwell plot) and the tangent plot (evaluated in this research) allows to rough estimate the buckling load for those cases (as in specimens 3, 5, 7 and 9) when the load history firstly reached the 5872 kN (1320 kip) of maximum axial capacity of the testing system.

Figure 5 shows the results of the application of the secant and the tangent plots from the data measured in these tests (specimens 3, 5, 7 and 9). In this figure, the blue thick lines represent a filtered and smoothed record of the raw data denoted by the green thin lines. Additionally, stated in this figure are the maximum load, $P_{max}$, applied in the test and the y-intercept of the secant plot ($P_s$, rough estimator of the $P_e$) and the tangent plot ($P_t$, rough estimator of the $P_n$ or $P_{cr}$); the points used for the calculation of the slopes and the extrapolated line to the y-intercept are included in these plots.

As observed in Figure 5, the smoothed experimental data do not exhibit a clear linear relation. This may be attributed to the influence of the second order terms in the series expansion solution. Nevertheless, this approach may be seen at a first approach to rough estimate the experimental axial load capacity in these specimens where the buckling load was not met during the test.

7
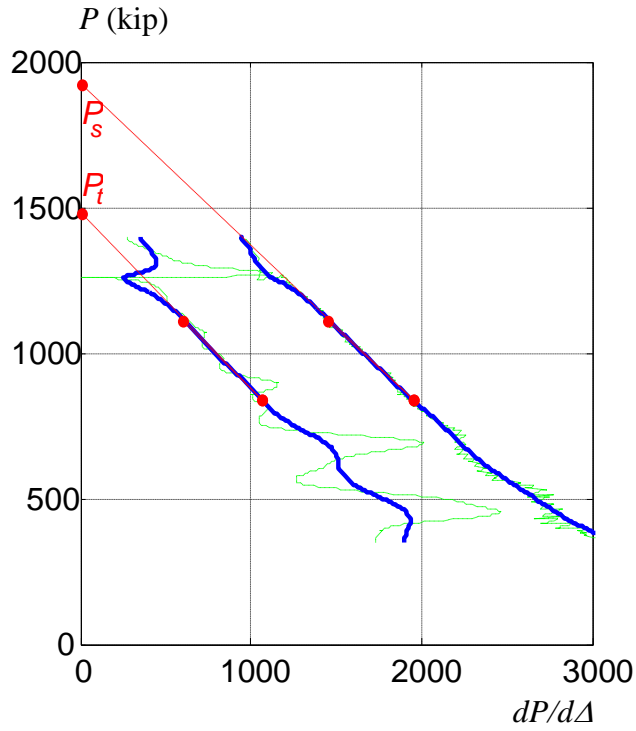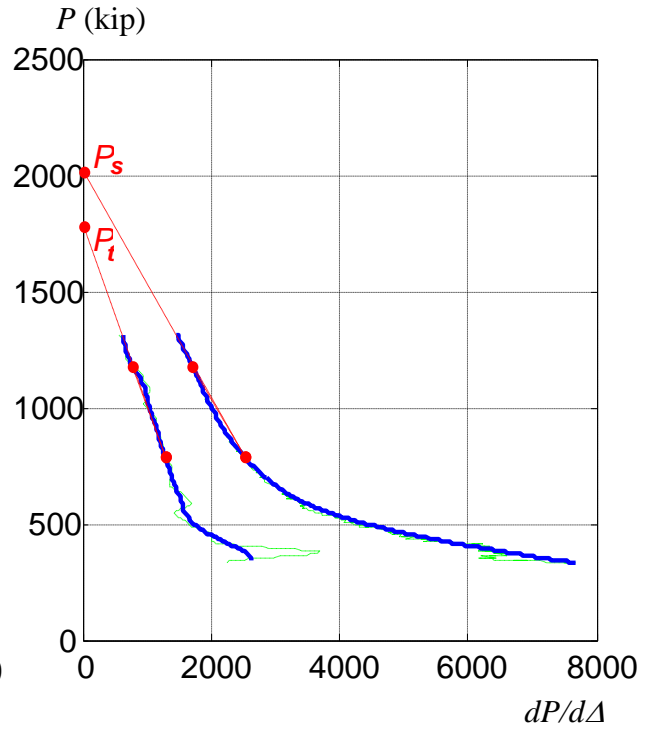
(a) Specimen 3

(b) Specimen 7
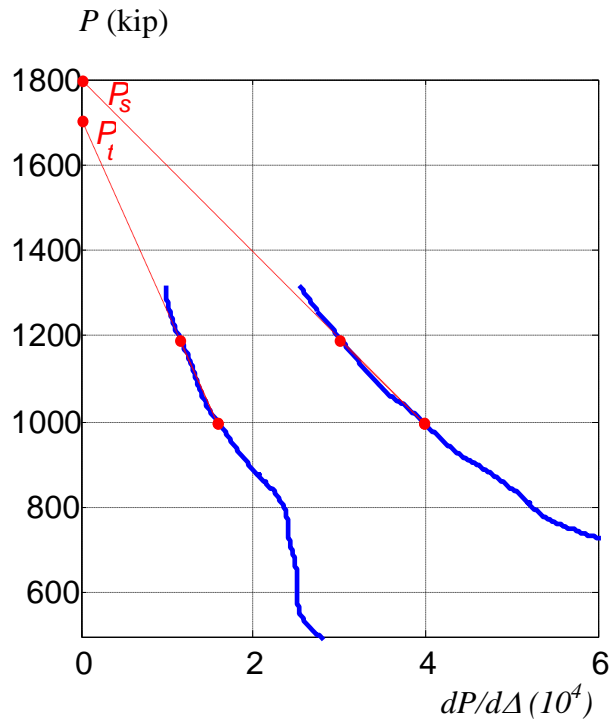
(c) Specimen 5
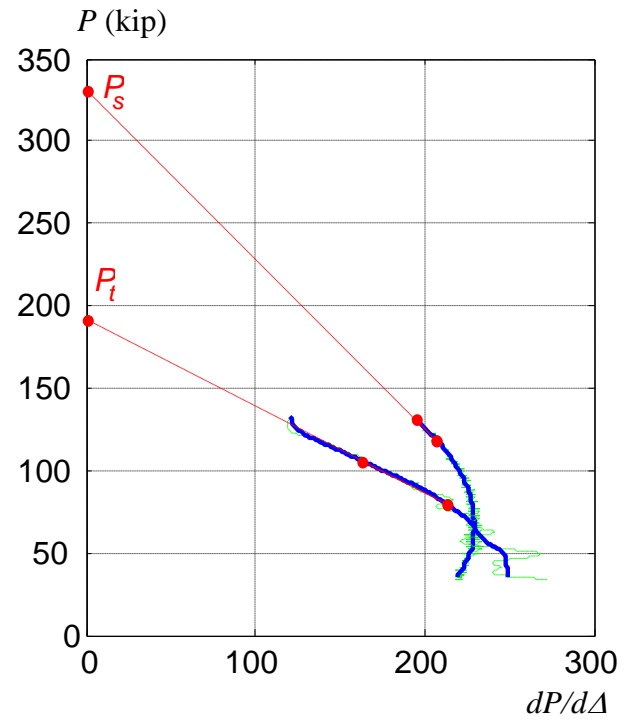
(d) Specimen 9

Figure 5. Application of the tangent and the secant form on the CFT specimens that did not buckle with the full compressive capacity of the MAST system

A summary of the buckling load capacities obtained from Figure 5 is shown in Table 2. In this table, $\lambda$ and $P_n$ are respectively the slenderness parameter and the buckling capacity calculated with the AISC (2016) Specifications, $P_{max}$ is the maximum experimental axial load applied on the specimens, $P_s$ is an estimator of the Euler load obtained with the secant plot, and $P_t$ is an estimator of the buckling load capacity, $P_n$, obtained with tangent plot.

Table 2: Summary of the maximum axial loads obtained from incomplete experimental data

| Specimen | $P_{max}$ (kN) | AISC (2016) | | | Southwell $P_S$ (kN) | $P_S / P_n$ ratio | Tangent $P_T$ (kN) | $P_T / P_n$ ratio |
|---|---|---|---|---|---|---|---|---|
| | | $\lambda$ - | $P_e$ (kN) | $P_n$ (kN) | | | | |
| 3 | 5872[a] | 1.10 | 8,664.2 | 6,295.5 | 8,531.7 | 1.355 | 6574.5 | 1.045 |
| 7 | | 1.36 | 10,646.4 | 9,088.9 | 9,007.6 | 0.991 | 7966.8 | 0.877 |
| 5 | | 0.91 | 11,196.0 | 6,528.0 | 8,006.8 | 1.227 | 7584.2 | 1.162 |
| 9 | | 1.07 | 13,370.1 | 9,513.4 | 14,679.1 | 1.543 | 8531.7 | 0.897 |

Note: [a] Maximum laboratory capacity to axial load.

## 5. Conclusions

This paper presented the application of two techniques that target the determination of the buckling critical load of composite concrete-filled steel tube (CFT) columns from incomplete or partial experimental axial load – lateral out-of-plumbness displacement ($P$-$\Delta$) data. The numerical techniques evaluated in this study are the secant approach (better known as the Southwell plot) and the tangent approach. The motivation of this study arises from the inability of a sophisticated laboratory system to reach the experimental peak buckling capacity of some full-scale composite CFT specimens. The two techniques are validated against numerical nonlinear analyses of composite CFT columns with different values of slendernesses and initial imperfections. The techniques were then used to estimate the axial capacity of four specimens that were tested experimentally. The evaluation with both the available experimental dataset and the parametric study confirms the scope and limitations of these two techniques. The application of the secant approach allows a more accurate determination of the critical load for composite CFT columns with capacity greater than that of the laboratory system in which they are tested.

## Acknowledgments

## References

AISC (2016). "Specifications for structural steel buildings. ANSI/AISC 360-16". American Institute of Steel Construction. Chicago, IL.

Hajjar, J. F., French, C. W., Schultz, A. E., Shield, C. K., Ernie, D. W., Dexter, R. J., Du, D. H., and Bergson, P. M. (2002). "A system for multi-axial subassemblage testing (MAST): initial developments." *Proceedings of the American Society of Civil Engineers Structures Congress*, Denver, Colorado, April 4–6, 2002, 313–314.

Horton, W. H., Cundari, F. L., and Johnson, R. W. (1971). "Applicability of the Southwell Plot to the Interpretation of Test Data Obtained from Stability Studies of Elastic Column and Plate Structures". *USAAVLABS Technical Report 69-32*. Department of the Army. Fort Eustis, VA.

Perea, T. (2010). "Analytical and Experimental Study on Composite Concrete-Filled Steel Tube Beam-Columns" *Ph.D. Thesis*, School of Civil and Environmental Engineering, Georgia Institute of Technology, Atlanta, GA.

Perea, T., Leon, R. T., Hajjar, J. F., Denavit, M. D. (2013). "Full-Scale Tests of Slender Concrete-Filled Tubes: Axial Behavior". *Journal of Structural Engineering*. ASCE. Special Issue: NEES 1: Advances in Earthquake Engineering. 139(7), pp. 1249-1262.

Timoshenko, S. (1961). "Theory of elastic stability". McGraw-Hill, New York.